Quantum Chemical Study of the Photocoloration Reaction in the Napthoxazine Series

F. Maurel,*,† J. Aubard,† P. Millie,‡ J. P. Dognon,§ M. Rajzmann,⊥ R. Guglielmetti,⊥ and A. Samat⊥

Laboratoire Interfaces, Traitements, Organisation et DYnamique des Systèmes (ITODYS), Université de Paris 7—Denis Diderot, UMR 7086, 1 rue Guy de la Brosse 75005 Paris, France, Laboratoire de Chimie Physique, UMR 8000, Bât. 350, Université Paris Sud, 91405 Orsay Cedex, CEA-Saclay, DSM/DRECAM/SPAM CNRS, URA 2453, Bât. 522, 91191 Gif sur Yvette Cedex, and Faculté des Sciences de Luminy, Université de la Méditerrannée, GCOM2, UMR 6114, Case 901-13288 Marseille Cedex 9, France

Received: September 2, 2005; In Final Form: February 21, 2006

Ab initio and semiempirical quantum mechanical calculations were performed to study the electronic spectra of spiroxazine photochromic compounds as well as the corresponding photoisomers. Ground-state geometries were optimized based on density functional theory (DFT). Excitation energies of the different forms were calculated using the time-dependent density functional theory (TD-DFT) method. Semiempirical calculations including configuration interactions were performed to detail the mechanism of ring opening in excited states. On the basis of the obtained potential energy profile, a complete mechanism of photocoloration able to clarify some experimental findings is provided. A correlation of the experimental quantum yield of photocoloration with the calculated properties as a function of substituent effects is proposed.

1. Introduction

Photochromic compounds exhibit reversible variations in color when exposed to specific light.[1] This property allows the use of these compounds in many applications. Mechanistically, photochromism exhibited by these compounds is due to a ring-opening electrocyclic reaction upon UV radiation and nonradiative deactivation to the ground-state potential energy surface (PES) to produce a mixture of isomers of merocyanines forms, i.e., colored species (Scheme 1)[1] which are thermally and/or photochemically revertible to the original closed form. Thermal ring closure at room temperature is responsible for the fading reaction.[1] Among the great variety of organic photochromic compounds, spironaphthoxazines (SNO) have attracted much attention owing to their good overall properties.[2] Particularly, the high fatigue resistance upon many cycles of opening−closing reactions makes these compounds very good candidates for potential applications.[3−7]

Because the duration of the primary process is very short, the ring-opening reactions have been studied in the vast majority of cases by using time-resolved spectroscopic techniques. In the pioneer studies, photochromism of spirooxazines was examined by nanosecond[8] and picosecond[9,10] transient absorption spectroscopy. These studies have suggested that the photochromic reaction which transforms the spiro form, via ring opening, to merocyanine isomers occurs within the laser pulse (i.e., below 10 ps) through the first excited state of the closed form. More recently, the use of femtosecond pulses allows some details about the ultrafast dynamics involved in the photochromic process to be provided.[11−13] Then, a relatively more precise ring-opening mechanism was proposed by Tamai and Masuhara[11] It was suggested that a primary photoproduct, showing an s-cis geometry (vide supra) and often called X in the literature, is formed immediately after the spiro carbon−oxygen bond cleavage within 700 fs. This first photoproduct evolves within 470 fs toward a metastable merocyanine isomer. Finally, quite metastable merocyanine rearranges to a more stable one on a time scale of several tens of picoseconds. A similar mechanism was also reported by Antipin et al.[12] following femtosecond time-resolved spectroscopic experiment. In this study, the characteristic time for the process of transient formation was typically estimated within 100−300 fs. Other work based on picosecond time-resolved resonance Raman (TR^3) spectroscopy suggests that the formation of photomerocyanines isomers occurs directly from the first excited state of spirooxazine populated by optical excitation[14] without s-cis intermediate participation on the time range above 50 ps. Surprisingly, in recent picosecond absorption and TR^3 spectroscopic studies, on related SNO compounds, it was claimed that such an intermediate participates in the ring opening in the 6−30 ps time range.[10] However, this was not confirmed by similar Raman experiments performed on a naphthoxazine compound, in which no such intermediate was detected in the time range of 5−100 ps.[15,16] In summary, although it is generally accepted that the C−O bond cleavage occurs in the first singlet excited state, and despite considerable experimental efforts using a great variety of time-resolved electronic absorption and vibrational spectroscopic techniques, conclusive evidence for a detailed excited-state ring-opening mechanism is still lacking. Particularly, the existence and the nature of the short-lived photoproduct formed just after the excitation is still questioned.

From a theoretical point of view, most studies were performed at the semiempirical level of calculations for excited states owing to the size of the compounds. Ground-state studies focused on the thermodynamic stabilities of the merocyanines isomers,[17] and recently the thermal coloration and decoloration of an SNO were studied by performing density functional theory (DFT)

* Corresponding author. Fax: 33 1 44 27 68 14. E-mail: maurel@paris7.jussieu.fr.
† Université de Paris.
‡ Université Paris Sud.
§ CEA-Saclay, DSM/DRECAM/SPAM CNRS.
⊥ Université de la Méditerrannée.

10.1021/jp054976f CCC: $33.50
Published on Web 03/22/2006

SCHEME 1

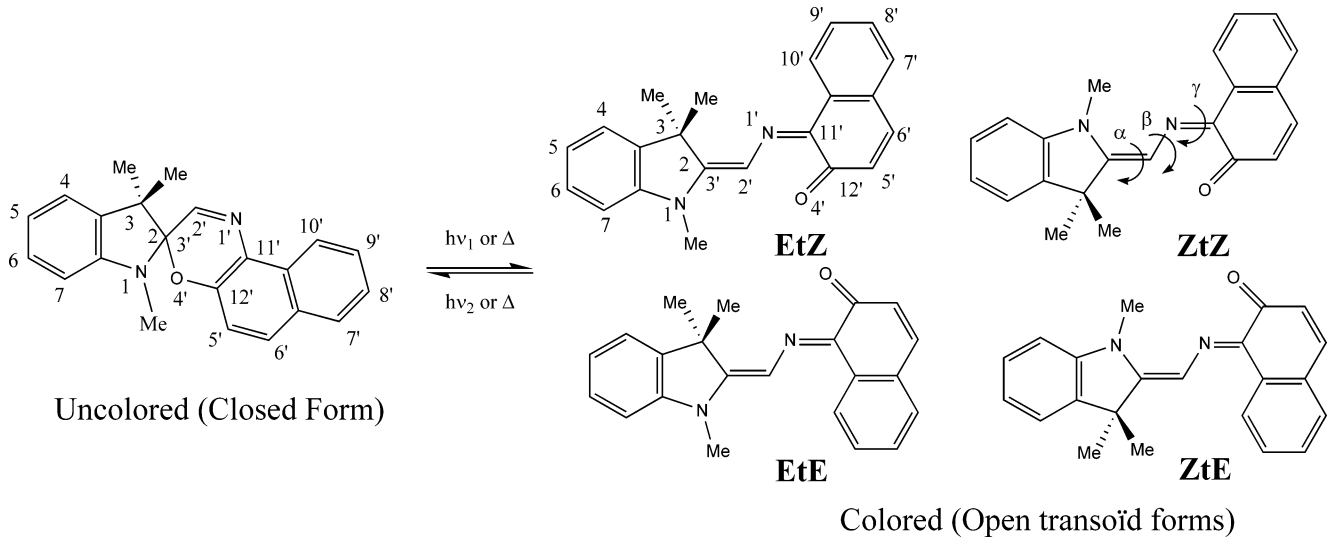

calculations.[18] In this last study, all feasible thermal reactions of ring closure as well as isomerization between merocyanine isomers have been calculated. Particularly, it has been shown that each of the ring-closure mechanism involves two steps (merocyanine → s-cis isomerization followed by C−O bond formation). These results provide an interpretation for the two-phase kinetics measurements of the fading reaction.[18] On the other hand, Celani et al. have considered the photoinduced ring-opening process for different models of molecules, closely related to usual photochromic compounds, using CASSCF methodology. Calculations for pyran, benzopyran, and aminopyran[19] models in the first excited state show that the ring-opening reaction proceeds with a very low barrier of activation. From the excited-state closed form, the system evolves on the excited-state surface until an opened structure region is reached. Finally, nonradiative deactivation to the ground state proceeds through a conical intersection. From this conical intersection, relaxation on the ground-state surface can occur toward two different minima, one corresponding to the initial closed form, the other to an open merocyanine isomer of tZ geometry (Scheme 1). This study provides a detailed description of the excited ring opening for the small size system. However, similar studies focused on the largest size compound for which a lot of experimental data were reported (such as absorption spectrum of the open form, quantum yield of photocoloration, kinetics of ring closure, and so on) are still not available.

In this paper, we report on a molecule of fundamental importance, the "parent compound", of a large family of naphthooxazinic photochromic compounds, i.e., SNO. SNO is a structure large enough to exhibit a rich and complicated photochemistry. The key point in the photochemistry of spirooxazine is the mechanism of formation of a photochromic transient that is born in its ground state from the excited closed form in an ultrafast process.[11] Unfortunately, this molecule is too large for a theoretical treatment at the excited-state level by application of the high-level ab initio quantum chemical methods such as CASSCF calculations. However, recent advances in electronic structure theory allow the calculation of excited-state energies and transition probabilities for medium-sized molecules within the ab initio methods. Examples include density functional response methods. At our best knowledge, none of these methods has been used to study the excited-state properties of spiroxazine photochromic compounds. Therefore, we combined the use of semiempirical calculations for excited-state geometries optimization with the time-dependent density functional theory (TD-DFT) for excitation energies. In this paper we present an exhaustive analysis of the ground state using the DFT method and low-lying singlet states of spiroxazine using both semiempirical and TD-DFT methods.

Despite considerable experimental and theoretical efforts, the detailed photochromic process of SNO has not been completely clarified. Although the transient absorption spectroscopy studies have reported long-lived and short-lived species during the ring-opening reaction, their characteristics as well as their role in the photochromic mechanism must be specified. Therefore, the main goals of this study are (i) to establish a general theoretical frame for the photocoloration process of a real photochromic compound which could be also applied for various photochromic series, i.e., spiropyran and 2H-chromene and (ii) to propose an explanation of the photocoloration quantum yield variation upon substituent effect.

2. Theoretical Calculations

Quantum chemical calculations were performed with the help of the Gaussian 98 suite of programs.[20]

To shed light on the ring-opening mechanism, we should determine some characteristic properties of the ground state as well as excited-states PESs. Particularly, it is necessary to calculate the minima, transition states connecting some minima, and if present, the crossing point between the different PESs under study. The determination of reliable geometric structures and energies for conjugated compounds is however a nontrivial quantum chemical task. The precise balance between double- and single-bond lengths (bond length alternation) in a conjugated system requires taking into account electron correlation. The importance of exchange energy for bond length alternation has been recognized,[21] and excellent results were obtained taking into account a part of the Hartree−Fock exchange in a hybrid DFT method. Therefore, the ground-state potential surface for ring opening was studied by using the hybrid B3LYP[22] functional with the 6-31G(d)[23] basis set.

The description of the excited-state potential surface at a very accurate ab initio level (like complete active space self-consistent field (CASSCF)) is beyond the capability of calculations for such a large system. Alternatively, semiempirical calculations using configuration interaction (CI) are proven to be useful to obtain the approximate wave function and molecular geometry

of the electronic excited states. However, it usually overestimates the energy differences between the excited and ground states. In comparison, the TD-DFT method currently cannot perform geometry optimization of the excited states, but it has been shown to be able to obtain very reliable vertical excitation energies for the low-lying states. Accordingly, two ways of calculating the excited-state energies were employed here. A coupled semiempirical RHF-AM1[24]/configuration interaction (AM1-CI) method using complete active space configuration interaction (CAS-CI) available in the AMPAC program[25] package was used for the optimization of the excited states. All singly and doubly excited configurations involving the seven highest occupied and seven lowest unoccupied orbitals were included in the CI expansion (CI = 7/7). This size of active space allows us to include all the orbitals involved in the photochromic mechanism, i.e., π and π^* orbitals as well as σ_{CO} and σ_{CO}^* orbitals. The applicability of the AM1-CI method has been extensively tested for conjugated molecules[26] and was found to reproduce qualitatively well the ground state and excited geometries. However, the spectroscopic results are not of comparable quality. It is found that AM1-CI calculations overestimate by more than 1 eV the maximum absorption for the colored forms (the maximum absorption transition is calculated at 363 nm instead of 567 nm experimentally). So, we calculate in a second step the vertical excitation using a modified version of CS-INDO[27]-CIPSI[28] or with TD-B3LYP method. The semiempirical CS-INDO-CIPSI framework has been especially modified in order to compute the excited states of large conjugated molecules.[29] Indeed, to get past severe limitations inherent to the calculations of electronic states in the case of a large conjugated molecule, the σ MOs (bonding and antibonding) are localized, while the π system is delocalized. As described in detail in ref 29, such a strategy allows one to reduce the number of two-electron integrals and the size of the CI matrix. Recent calculations using this strategy have been shown to be very successful in predicting the maximum absorption of the colored form for photochromic compounds.[30] Vertical excited-states calculations were carried out on the DFT geometries of the closed and open isomers. Excitation energies were also calculated by the TD-DFT method.[31] TD-DFT calculations using the B3LYP functional and the 6-31G basis set were found to be a good compromise between computational time and accuracy. Particularly, this procedure of calculations correctly reproduced the absorption spectrum of the initial form (vide supra).

3. Results and Discussion

3.1. Spectroscopic Properties of the Closed Form. The chiral spiro carbon C_2 (or $C_{3'}$) (see Scheme 1) of SNO leads to two enantiomeric forms of the same energy, named CF(R) and CF(S), whose optimized geometries are depicted in Figure 1.

The central spiro carbon atom forces the two conjugated fragments to be in perpendicular planes. Therefore, the absorption spectrum of the spiro form is, if we neglect in the first approximation charge-transfer (CT) states, the sum of the spectra of the individual moieties,[32] i.e., the indoline and naphthoxazine moieties. To provide a detailed analysis of the first excited states of the closed form as localized excitations (LE) on each fragment or CT states, we first performed a study of the SNO diagram orbital. In Figure 2, the orbitals of indoline and naphthalene moieties constituting the molecule were correlated to the orbitals of SNO. This correlation was done by comparison of the shape and energies of the SNO orbitals with those of the fragments. In that way the orbital of SNO can be easily built from the orbitals of each fragment.

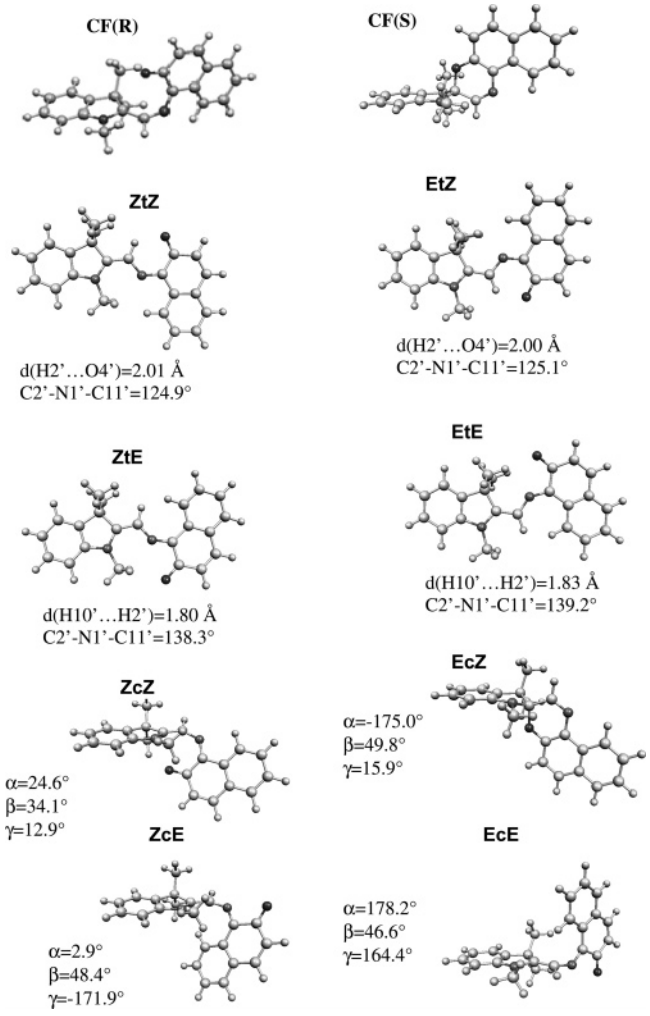

Figure 1. B3LYP/6-31G(d)-optimized geometries of the closed forms, CF(R) and CF(S), and open forms (s-trans and s-cis isomers).

From inspection of Figure 2, it is clear that orbitals of each fragment do not significantly interact in the closed form geometry. For instance, the HOMO of the spiro form corresponds to the HOMO of the indoline compound, while the LUMO is connected to the more acceptor fragment, i.e., naphthoxazine. The HOMO → LUMO transition corresponds mainly to a CT transition from indoline to naphthoxazine. For symmetry reasons, this transition should have a very low oscillator strength. The three lowest unoccupied orbitals LUMO, LUMO + 1, and LUMO + 2, as well as HOMO − 1 and HOMO − 2, are localized exclusively on the naphthoxazine fragment suggesting that the lowest vertical excitation of significant intensity is built on almost LE on naphthoxazine. Orbitals localized on indoline are H − 3, H − 6, L + 3, and L + 4. As the energy differences between indoline-localized orbitals are much larger, it is anticipated that localized indoline excitation will be found at higher energy than that of localized naphthoxazine ones. Moreover, comparison between vertical excitation energies of SNO with those of individual fragments allows an assignment of these transitions as localized or CT. The results from the TD-DFT and CS-INDO-CIPSI approaches for the singlet excited states of the enantiomeric closed forms of spiroxazine are presented in Table 1.

Both methods reproduce very well the observed electronic transitions in the absorption spectrum of SNO.[33] In accordance with the correlation diagram, calculations show that the lowest transition is of a $\pi-\pi^*$ nature and is dominated by the HOMO

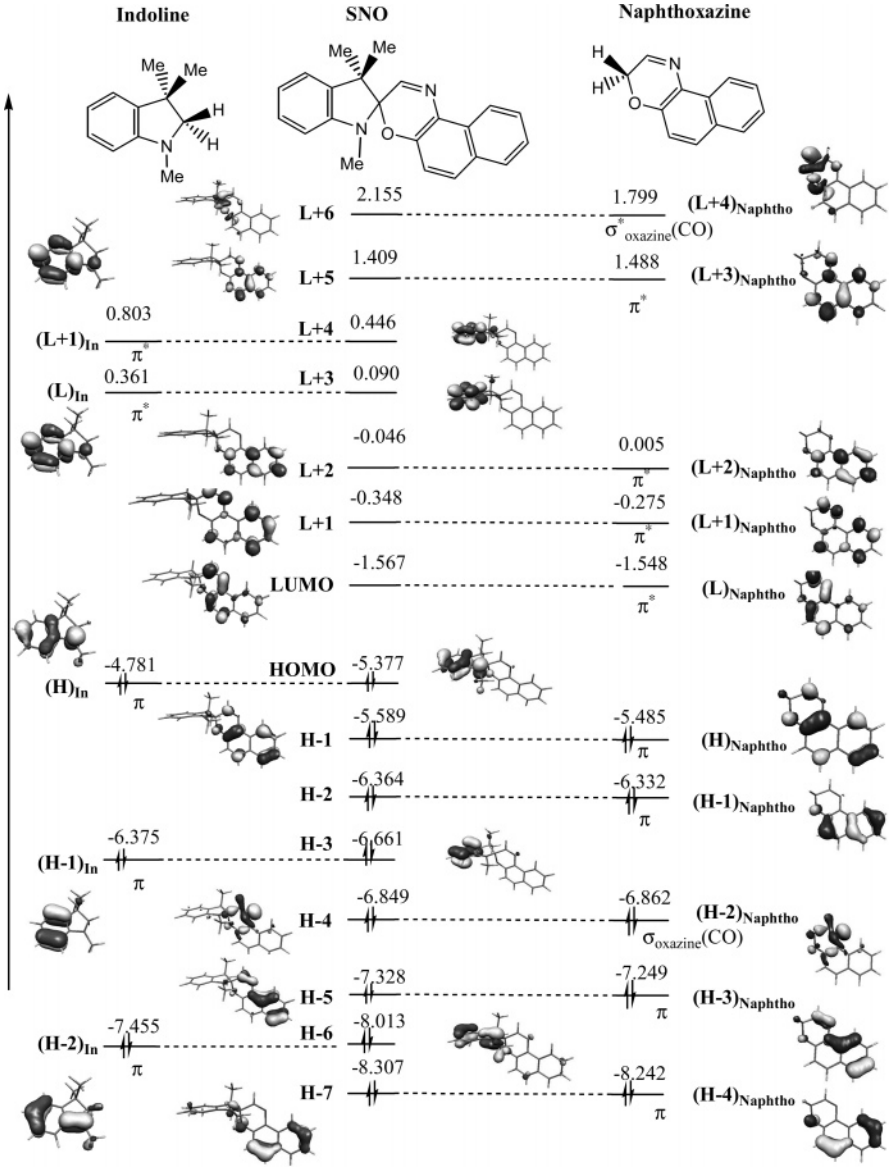

Figure 2. Diagram of monoelectronic orbitals of indoline, naphthoxazine, and their spiro form in SNO (energies are in eV).

TABLE 1: Vertical Excitation Wavelengths, λ (in nm), and Oscillator Strengths, *f*, Predicted for the First Singlet Excited States of CF(R) in the Gas Phase with CS-INDO-CIPSI (A) and TD-DFT (B) Methods[a]

	SNO						fragment	
	calcd				exptl[b]			
state	λ		*f*	description	λ	intensity	indoline	naphthoxazine
	A	B						
S_1	353	389	0.0060	H → L (CT)	369	W		
S_2	322	343	0.0150	H − 1 → L (LE)	345	M		353
S_3	315	306	0.0051	H − 4 → L + H − 2 → L (LE)	317	M		308
S_4	290	296	0.0042	H − 4 → L − H − 2 → L (LE)	297	M		298
S_5		277	0.0005	H → L + 1 (CT)				
S_6		271	0.0003	H − 3 → L (LE)		W		270
S_7		266	0.0013	H − 1 → L + 1 (CT)				
S_8		261	0.0048	H → L + 2 + H → L + 3 (LE)			279	
S_9		255	0.0084	H → L + 2 − H → L + 3 (CT)				
S_{10}		250	0.0097	H − 5 → L − H − 2 → L + 1 + H − 1 → L + 2 (LE)				253
S_{11}		239	0.0055	H − 1 → L + 3 (CT)				
S_{12}	238	235	0.0724	H − 5 → L (LE)	235	S		234
S_{13}	203	230	0.0417	H → L + 4 (CT)	235	S	236	

[a] The B3LYP/6-31G(d) S_0 geometry is used to calculate the excited states. [b] Ref 32.

→ LUMO single excitation. Since the HOMO and LUMO orbitals are localized mostly on different rings, this electronic transition has a very weak oscillator strength ($f = 0.006$) and might be therefore assigned to the weak shoulder at 369 nm in the experimental UV spectrum.[33] The next three lowest singlet states correspond to local excitation of the naphthoxazine

TABLE 2: Vertical Excitation Wavelengths, λ (in nm), and Oscillator Strengths, *f*, Predicted for the First Five Singlet Excited States of the Open Forms (s-trans and s-cis) in the Gas Phase with the TD-DFT and CS-INDO-CIPSI Methods

		EtZ		ZtZ		EtE		ZtE		exptl[a,b]
transition	description	λ	*f*	λ	*f*	λ	*f*	λ	*f*	λ
$S_0 \rightarrow S_1$	$\eta_o\pi^*$									
TD-DFT		553	0.0	556	0.0	497	0.023	504	0.027	
CS-INDO-CIPSI		612		621		563		557		
<chgrow;lp;4q> $S_0 \rightarrow S_2$	$\pi\pi^*$									567
TD-DFT		475	0.051	475	0.051	455	0.022	458	0.018	
CS-INDO-CIPSI		547		547		513		533		
<chgrow;lp;4q> $S_0 \rightarrow S_3$	$\pi\pi^*$									
TD-DFT		402	0.007	401	0.007	392	0.011	398	0.010	
CS-INDO-CIPSI		371		374		397		387		
<chgrow;lp;4q> $S_0 \rightarrow S_4$	$\pi\pi^*$									
TD-DFT		333	0.002	332	0.002	374	0.003	379	0.003	
CS-INDO-CIPSI		358		259		325		334		
<chgrow;lp;4q> $S_0 \rightarrow S_5$	$\pi\pi^*$									
TD-DFT		320	0.000	320	0.000	328	0.023	330	0.022	
CS-INDO-CIPSI		306		309		318		320		

		EcZ		ZcZ		EcE		ZcE	
transition	description	λ	*f*	λ	*f*	λ	*f*	λ	*f*
$S_0 \rightarrow S_1$	$\eta_o\pi^*$								
TD-DFT		755	0.007	628	0.008				
CS-INDO-CIPSI		834		877		985	985	808	808
<chgrow;lp;4q> $S_0 \rightarrow S_2$	$\pi\pi^*$								
TD-DFT		422	0.025	425	0.034				
CS-INDO-CIPSI		500		573		500	500	479	479
<chgrow;lp;4q> $S_0 \rightarrow S_3$	$\pi\pi^*$								
TD-DFT		412	0.007	404	0.002				
CS-INDO-CIPSI		420		497		413	413	387	387
<chgrow;lp;4q> $S_0 \rightarrow S_4$	$\pi\pi^*$								
TD-DFT		366	0.003	348	0.002				
CS-INDO-CIPSI		379		390		382	382	371	371
<chgrow;lp;4q> $S_0 \rightarrow S_5$	$\pi\pi^*$								
TD-DFT		348	0.009	339	0.009				
CS-INDO-CIPSI		369		380		348	348	349	349

[a] Ref 44. [b] Ref 8.

moiety. Indeed, three $\pi \rightarrow \pi^*$ transitions of medium intensity and localized on the naphthoxazine moiety are calculated at 343, 306, and 296 nm with the TD-DFT method and are assigned to the experimental absorption bands at 345, 317, and 297 nm, respectively (Table 1). In the high-energy side of the spectrum, two transitions are localized on indoline at 261 nm ($f = 0.0048$) and 230 nm ($f = 0.0417$). These values are in good agreement with experimental electronic transitions measured for indoline at 287 and 237 nm[34] and appear to correspond to similar transitions of aniline. We also calculated a strong $\pi \rightarrow \pi^*$ transition at 235 nm ($f = 0.0724$) which is localized on the naphthoxazine moiety. It should be noted that the first excited state involving significant contribution of the σ^*_{CO} antibonding orbital corresponds to a very high energy excited state, i.e., S_{13} (this state is described mainly by a single excitation involving H $\rightarrow$ L + 4 where L + 4 orbitals are a σ^*_{CO} antibonding combined with a π antibonding orbital localized on the indoline fragment). Following this study it can be concluded that the lowest energy excited state which significantly absorbs is S_2. This excited state is of the $\pi-\pi^*$ type localized on the naphthoxazine and then cannot involve the σ^*_{CO} antibonding orbital. Therefore, the $S_0 \rightarrow S_2$ vertical excitation cannot lead to a direct C−O bond cleavage. In most experimental studies, the excitation of SNO is performed using a wavelength smaller than 300 nm, typically 250 nm. In these conditions, we can assume that the S_2 excited state is initially populated by UV absorption. Following this absorption, ultrafast nonradiative deactivation to the first excited state occurs. This nonradiative deactivation is favored by the small energy gap between the two first excited states. As a consequence, the study of the excited ring-opening mechanism will be restricted to the calculations of the S_1 and S_2 PES.

3.2. Spectroscopic Properties of the Open Form. In the open forms, due to the structure of the conjugated chain between the indoline and naphthalene moieties, eight isomers are possible of either cis or trans configuration of the $C_{3'}-C_{2'}$, $C_{2'}-N_{1'}$, and $N_{1'}-C_{11'}$ bonds. All these open isomers can be divided in two groups: either the central $C_{2'}-N_{1'}$ has a trans or a cis configuration (Figure 1). The s-trans isomers, i.e., ZtZ, EtE, ZtE, and EtZ isomers (namely, the classically reported ones in other studies [33]CTC, TTT, CTT, and TTC, respectively) have nearly planar (C_s symmetry for ZtZ and EtZ and C_1 symmetry for EtE and ZtE isomers) geometry and absorb in the visible region. Due to the steric repulsion between the naphthalene hydrogen and conjugated bridge, the s-cis, i.e., ZcZ, EcE, ZcE, and EcZ isomers, strongly deviate from planarity (Figure 1) and thus mostly absorb in the UV region and only weakly in the near-IR domain. We first discuss the spectroscopic properties of s-trans isomers.

The first lowest singlet vertical excitations of the s-trans (colored) isomers are gathered in Table 2. The S_1 state is a $\sigma \rightarrow \pi^*$ state in which an electron of the σ orbital localized on the oxazine ring (this orbital is mainly a combination of the two lone pairs of the oxygen and nitrogen atoms) is promoted to the lowest unoccupied π^* (LUMO) orbital. Owing to the symmetry, this transition is forbidden and associated to negligible oscillator strength in the planar geometry. The $S_0 \rightarrow S_2$ transition for more stable isomers, i.e., EtZ and ZtZ, are both calculated at 547 nm with the CS-INDO-CIPSI method which is in good agreement with experiment ($\lambda_{S0\rightarrow S2} = 567$ nm in

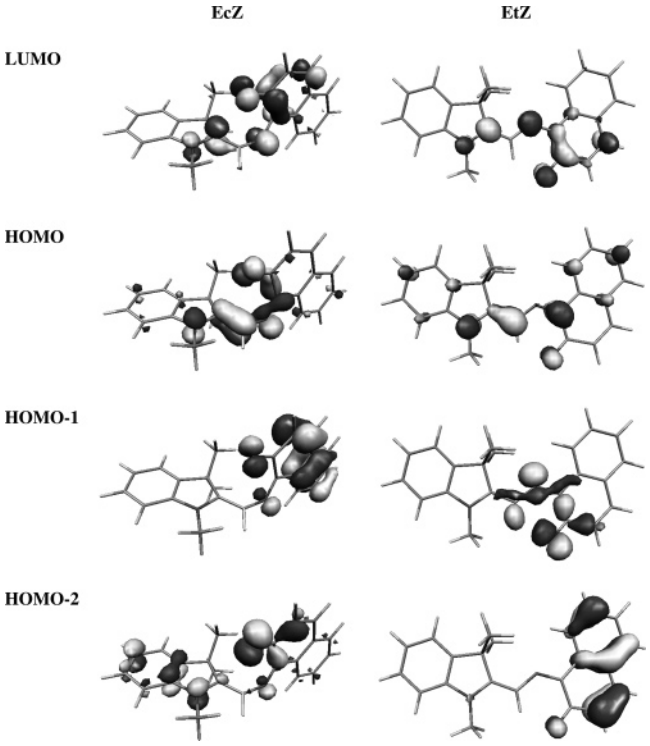

Figure 3. Kohn−Sham molecular orbitals involved in the electronic transitions of interest in the merocyanine forms (EcZ and EtZ) calculated with the B3LYP/6-31G(d) method.

nonpolar solvent[8]). The $S_0 \rightarrow S_2$ transition is mainly a $\pi \rightarrow \pi^*$ excitation (90% to the single HOMO → LUMO). As can be seen in Figure 3, these two orbitals are localized on the bridge joining the indoline and naphthoxazine moieties. Therefore, this transition looks like the lowest allowed singlet of polyene systems and, accordingly, has a very large oscillator strength ($f = 0.051$).

The $S_0 \rightarrow S_2$ excitation energies of EtE and ZtE are slightly blue shifted (513 and 533 nm, respectively) compared to those of ZtZ and EtZ. This shift can be explained by invoking two reasons. First, the geometries of EtE and ZtE are found to be slightly nonplanar which leads to loss of aromaticity and increases the HOMO−LUMO energy gap. The existence of a hydrogen bond between $H_{2'}$ and $O_{4'}$ in EtZ and ZtZ can be also, to a large extent, responsible for the bathochromic shift of the strongest allowed $S_0 \rightarrow S_2$ transition. Indeed, analysis of the orbitals involved in the transition indicates that the change in absorption wavelength is related to the change of orbital energy.[35] For instance, the HOMO−LUMO gap is 6.80 eV for full planar EtE and decreases to 6.55 eV for EtZ isomer.

S_2 excitation energies of the merocyanine form are too high at the TD-DFT level (Table 2). It is difficult to find an explanation for such failure of the TD-DFT method. However, most likely, the origin of the discrepancy lies in the inherent limitations of the TD-DFT method as reported for electronic states involving transitions between MOs localized in two remote from each other spatial regions (CT excitations).[36] This is apparently the case when SNO merocyanine is excited in the S_2 state. It could be also noted that a strong bathochromic shift is reported for maximum absorption in the colored forms of SNO when the polarity of the solvent increases. Therefore, considerable improvement in calculating the electronic excitation is attained if we consider the solvent effect. We calculated the first three lowest transition energies for the EtZ isomer in solution (Table 3) by using a continuum solvation model based on the self-consistent reaction field (SCRF).[37] A strong bathochromic shift from 475 to 546 nm is calculated for the $S_0 \rightarrow S_2$ transition when going from gas to acetonitrile solution, while no significant shift is calculated for the two other transitions. This suggests a strong stabilization of the highly polar second excited state by the polar solvent.

TABLE 3: Vertical Excitation Wavelengths, λ (in nm), and Oscillator Strengths, *f*, Predicted for the First Three Singlet Excited States of the EtZ Open Form (s-trans) in Solvent with the TD-DFT Method

		EtZ		exptl[a,b]
transition	description	λ	f	λ
$S_0 \rightarrow S_1$	$\eta_o\pi^*$			
gas		553	0.00	
acetonitrile		556	0.0	
$_0 \rightarrow S_2$	$\pi\pi^*$			567
gas		475	0.0051	
acetonitrile		546	0.075	595−600
$S_0 \rightarrow S_3$	$\pi\pi^*$			
gas		402	0.0073	
acetonitrile		411	0.009	

[a] Ref 44. [b] Ref 8.

The s-cis isomers, i.e., ZcZ, EcZ, ZcE, and EcE, exhibit a more complex calculated spectrum. Since the geometry of each isomer strongly deviates from planarity it allows some mixing between σ and π orbitals. Table 2 lists the calculated vertical energies for the first five excited states by two different methods. Due to the nonplanar conformation in all of these isomers, significant overlap can occur between the lone pairs on the nitrogen and oxygen atoms and the π orbitals located on the naphthoxazine moiety. For example, interaction between frontier orbitals raises the energy of the HOMO while decreasing such of the LUMO. This leads to a low-energy transition in the IR domain (the $S_0 \rightarrow S_1$ electronic transition calculated using the TD-DFT method is found at 755 and 628 nm for the EcZ and ZcZ isomers, respectively).

The open forms show contrasted properties: either the central $C_{2'}-N_{1'}$ has a cis or trans configuration. The most stable s-trans isomers, EtZ and ZtZ, strongly absorb in the visible while s-cis isomers show two main transitions in the UV and IR domains. In the following, we restricted our discussion to the two most stable isomers of each group, i.e., the EtZ and ZtZ s-trans and ZcZ and EcZ s-cis isomers. Indeed, it was established from previous experimental[38] and theoretical[18] studies that the coloration process leads to a mixture of these two s-trans isomers, while the s-cis are found to be intermediate on the ring-opening mechanism (vide supra).

3.3. Ring-Opening Mechanisms. Time-resolved spectroscopic techniques have shown that the formation of the colored merocyanine forms occurs in less than a few picoseconds. This means that even if the system evolves on the excited-state surface just after the UV excitation, fast deactivation to the ground-state surface should occur. Therefore, we first analyze the ground-state surface which determines the relaxation process a few picoseconds after the excitation of the closed form. In addition, the fading reaction, i.e., the ring-closure process, is entirely governed by the ground-state behavior.

3.3.1. Ground-State Surface. The topology of the ground-state surface that connects the closed forms (i.e., CF(R) and CF(S)) of SNO to the more stable merocyanines, i.e., ZtZ and EtZ, respectively, was explored by B3LYP/6-31G hybrid density functional calculations. The ring-opening profile was obtained by lengthening step by step the C−O bond while all the others parameters were fully optimized. Figure 4 sums up the results for the thermal ring opening of the two enantiomeric forms CF-

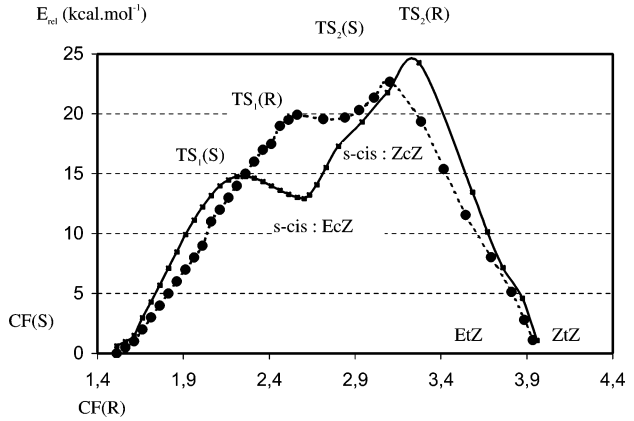

Figure 4. Ground-state surface for ring opening from CF(R) (solid line) and CF(S) (dashed line) enantiomeric closed forms (B3LYP/6-31G).

(R) and CF(S) (see Figure 1). Similar results were obtained using the same methodology but smallest basis set in a previous study.[18]

The calculations show that the ring opening of each closed form proceeds in two steps. The first step connects the closed form with an s-cis type intermediate (ZcZ or EcZ depending the initial stereochemistry of the closed form) through the $C_{3'}-O_{4'}$ bond cleavage transition state (TS_1(R) and TS_1(S)). The second stage consists of bond rotation around the central $C_{1'}-N_{2'}$ bond to obtain the final planar merocyanine forms, via TS_2(R) and TS_2(S). Similar mechanistic pathways were also reported for related photochromic compounds in the spiropyran series.[39] The overall activation barriers for the ring-opening reaction are found to be 22 and 25 kcal·mol^{-1} in reasonable agreement with experiment (23 kcal·mol^{-1}), while the overall reaction is slightly endothermic (5 kcal·mol^{-1}) which is also consistent with the thermal fading. The barrier of activation of $C_{3'}-O_{4'}$ bond cleavage is found similar for both closed forms (15 and 19 kcal·mol^{-1} from CF(R) and CF(S), respectively). The most change between both profiles comes from the higher bond rotation energy barrier for ZcZ (11.2 kcal·mol^{-1}) than for EcZ (2.2 kcal·mol^{-1}).

3.3.2. Ring Opening in Excited States. The excited ring-opening reaction could proceed via either a singlet or triplet excited state.[40] However, it has been already reported that the merocyanine formation is insensitive to the use of oxygen as a triplet quencher and thus that the reaction must involve the singlet manifold.[8,41] Recently, it was demonstrated that the photochromism of SNO is dominated by the singlet manifold, even with nitro substitution.[42] So we explore only the first (S_1 and S_2) singlet excited-state PESs. Two different procedures were used to obtain the excited state energetic profile. In the first type of calculations, geometries and energies were calculated using the AM1 Hamiltonian with CI. To properly describe the system in the region of bond breaking which can have some biradical character, we chose the restricted open shell formalism. Although CASSCF calculations would be suited, such formalism provides a better zero-order wave function than the restricted Hartree−Fock approach. The minimal energy path was obtained from CF(R) and CF(S) geometries by varying step by step the C−O bond distance while all the other parameters were fully optimized. For the second type of calculations, vertical excitation energies were calculated with the TD-DFT method and using the DFT ground-state optimized geometries. The obtained curves for CF(R) ring opening are shown in Figure 5, parts a and b, using the AM1-CI and TD-DFT methods, respectively. A similar

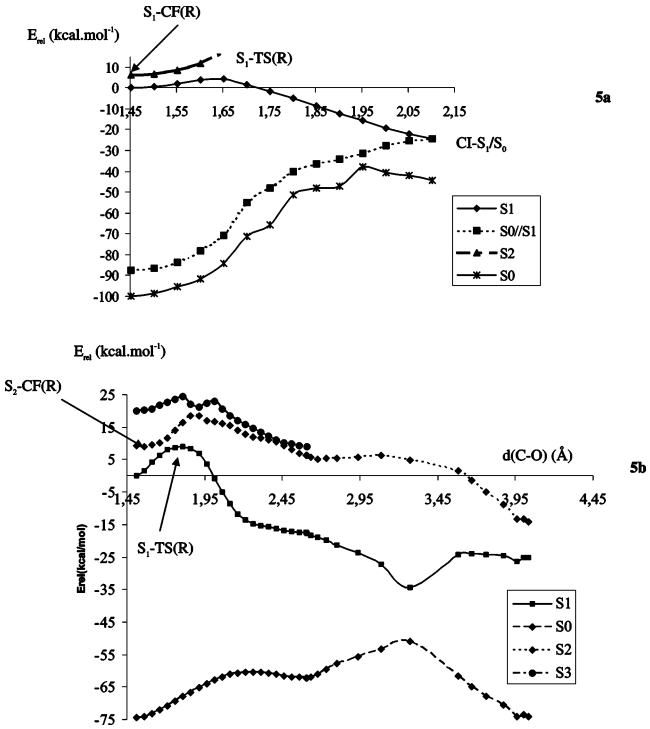

Figure 5. Potential energy profile for $C_2-O_{4'}$ bond dissociation obtained by using AM1-CI (a) and TD-DFT calculations (b) (the energy, in kcal·mol^{-1}, is taken relative to that of the closed form excited-state minimum, S_1-CF(R)).

energetic profile can be obtained starting from the other enantiomeric form CF(S).

3.3.2.1. S_1 PES (AM1-CI Results). We first discuss the AM1-CI results. From the Franck−Condon geometry, the system relaxes to its minimum energy conformation, namely, S_1-CF-(R). As expected, the C−O bond distance is not affected by the electronic excitation which involves the π system. By the lengthening of the C−O bond, the system reaches a transition state, S_1-TS(R), for a C−O distance of 1.66 Å (AM1-CI). The corresponding barrier for ring opening is about 4.3 kcal·mol^{-1} (this barrier of activation would certainly be smaller at a higher level of calculations[19]). After reaching the S_1-TS(R) transition state, the excited state evolves to the ring-opened region of the PES and a strong decrease in the potential energy of the S_1 state is calculated as the C−O bond is elongated. The photochemical ring opening reaches a pericyclic geometry where the S_1-S_0 gap is negligible. Hence, these calculations suggest that relaxation of the ring-opening excited state to the ground state involves a crossing between the S_1 and S_0 states (CI-S_1/S_0). Although we have not characterized the crossing point as a conical intersection thus far, this result is in good agreement with CASSCF calculations performed on a small model such as 2H-benzopyran[19] and the simplest related molecule such the oxazine ring (vide supra). The corresponding geometry is depicted in Figure 6 and shows a broken $C_2-O_{4'}$ bond, length of 2.10 Å with an almost perpendicular arrangement of the two conjugated rings: $\alpha = 66°$ while all the other dihedral angles along the conjugated chain are close to 0°.

In this geometry, the plane of the terminal carbon C_2 of the oxazine ring is twisted by almost 90° compared to the naphthoxazine molecular plane. In the CI-S_1/S_0 crossing point, the S_1 state corresponds to a $\pi-\pi^*$ state where the π orbital is localized on the naphthoxazine, while the antibonding π^* orbital is mainly localized on the C_2 center (see Figure 7).

Therefore, degeneracy arises because the radical centers do not interact with each other and with the π state on naphthox-

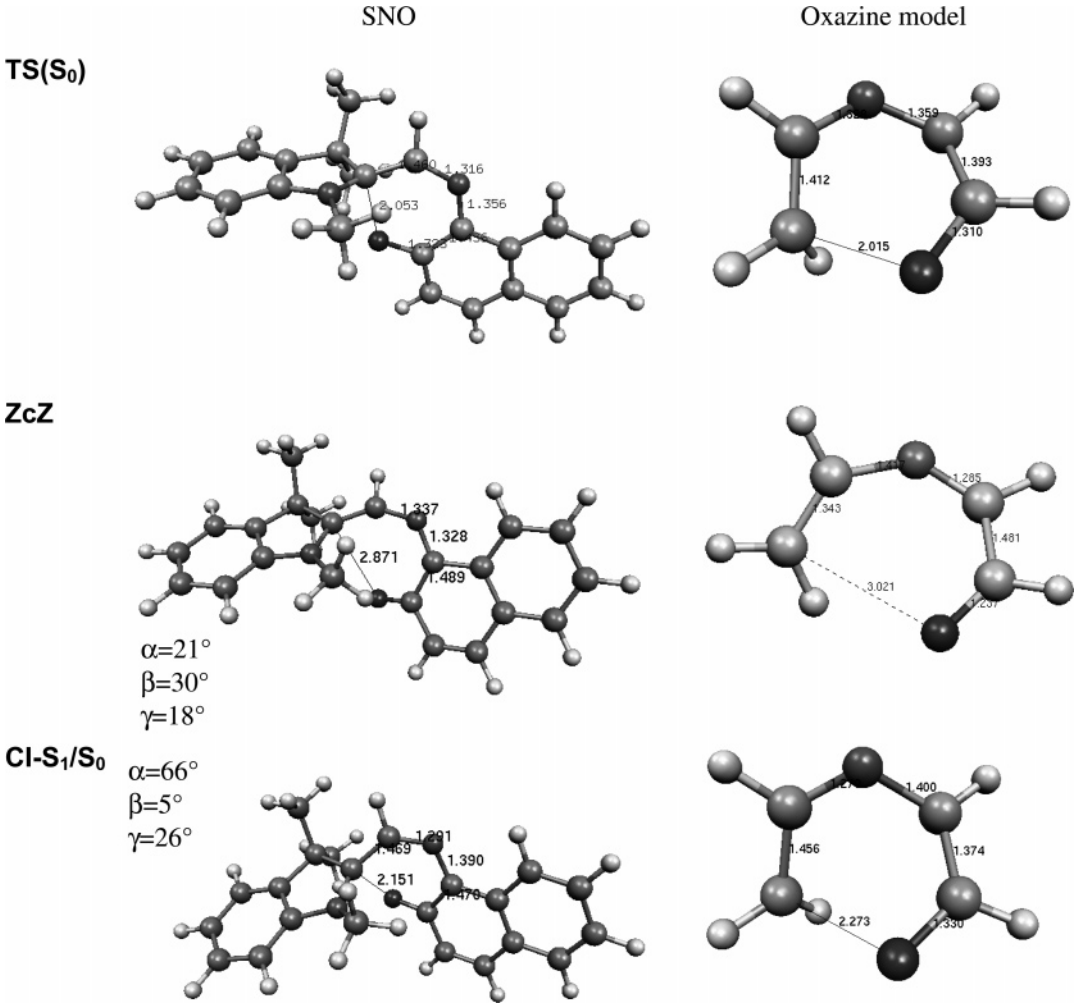

Figure 6. Structures of the ground-state ring-opening transition state ($TS(S_0)$), the ZcZ s-cis isomer, and the conical intersection $CI\text{-}S_1/S_0$ calculated at AM1-CI-ROHF for SNO and CASSCF(8,7) for the oxazine model.

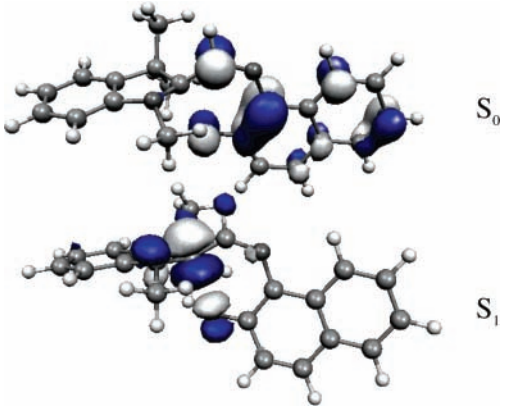

Figure 7. Low-lying $S_1(n-\pi^*)/S_0$ intersection in SNO ring opening.

azine. The S_1/S_0-CI geometry is shown in Figure 6 together with that of the minimum s-cis (ZcZ) and the transition state for the thermal ring-opening/closing $TS(S_0)$ (calculated by the same method). Subsequent geometry optimization of the S_0/S_1 crossing geometry in the ground state leads to the s-cis isomer, i.e., ZcZ. The corresponding relaxation path is obtained by increasing its $C_{2'}-N_{1'}$ and $C_{11'}-C_{12'}$ bond lengths and decreasing its $C_{3'}-C_{2'}$, $N_{1'}-C_{11'}$, and $C_{12'}-O_{4'}$ bond lengths (see Figure 6). However, it can been seen that the S_0-S_1 crossing state geometry shows great similarities with the thermal transition state for ring-opening/closing $TS_0(R)$; therefore, relaxation toward the initial closed form could not be excluded. The above result indicates a possible bifurcation of the reaction after passage through the conical intersection into two valleys, one leading to the initial closed form CF(R), the other to the full cleavage of the C−O bond to yield eventually the s-cis isomer. The partitioning ratio is expected to be more or less 1:1 for comparable probability for deactivation of S_1/S_0-CI to either the CF(R) or ZcZ ground states.

3.3.2.2. S_1 PES Calculated with the TD-DFT Method. The full energetic profile for ground state and excited states starting from CF(R) and calculated using the DFT method are displayed in Figure 5b. The beginning of the excited-state energy profile is quite similar to that obtained using AM1-CI methodology. After avoided crossing between S_1 and S_2 obtained for very weak elongation of the C−O bond, the S_1 curve showed an energy barrier with a maximum located for a C−O bond length of 1.70 Å. The calculated excited energy barrier for C−O cleavage is only 5 kcal·mol^{-1} which is very close to the AM1-CI value. From the excited-state transition state, the S_1 energy strongly decreases until the C−O bond elongation of 2.25 Å. The potential energy profile was not investigated for further C−O elongation using this method. Indeed DFT is a single reference method and therefore is not recommended to describe regions of the PES such as conical intersections where the two states should be described with equal quality.[43]

3.3.2.3. CASSCF Calculations Restricted to the Oxazine Model. To confirm the existence of the conical intersection located on the ring-opening pathway and then establish a

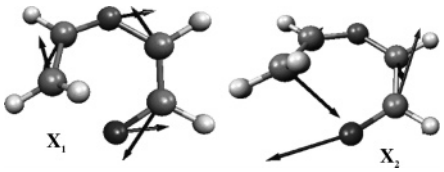

Figure 8. Nonadiabatic coupling $\mathbf{X_1}$ and gradient difference $\mathbf{X_2}$ vectors for the S_1/S_0 conical intersection of the oxazine model (calculated using the CASSCF(8,7)/6-31G method).

possible relaxation from the S_0/S_1 conical intersection on the PES ground state toward the closed form or s-cis intermediate, we carried out CASSCF calculations on a model restricted to the oxazine ring. Although this model molecule is rather simple, the ring-opening/closing electrocyclic reaction is representative of the mechanism involving in the largest size-related molecule. Excited-state CASSCF geometry optimization of this compound in the first excited state leads to a spontaneous ring opening toward an S_1/S_0 conical intersection. By contrast with the AM1 calculations performed on the SNO, the excited-state ring opening is barrierless. The optimized geometry of this S_1/S_0 conical intersection is shown in Figure 6. The nature of this conical intersection in terms of the geometrical variables can be easily understood by using the nonadiabatic coupling ($\mathbf{X_1}$) and gradient difference ($\mathbf{X_2}$) vectors. They define the directions of movements which will lift the degeneracy. The calculated nonadiabatic coupling vector and gradient difference vector for the ring-opening conical intersection point are shown in Figure 8, parts a and b, respectively. The nonadiabatic vector, $\mathbf{X_1}$, is dominated by a motion leading to a contraction of the $N_{1'}-C_{11'}$, $C_{3'}-C_{2'}$, and $C_{12'}-O_{4'}$ bonds. These geometric variations are similar to those calculated for the relaxation of SNO from the S_1/S_0 crossing to the s-cis ground-state geometry. The gradient difference vector, $\mathbf{X_2}$, is mainly dominated by a motion in the forming $C_{3'}-O_{4'}$ bond leading to the initial closed form. Therefore, analysis of nonadiabatic coupling and gradient difference vectors confirms a possible deactivation to the ground-state PES toward the initial closed form or s-cis open isomer.

From the s-cis isomer, the continuation of the reaction toward the merocyanine form on the ground state involves cis−trans isomerization around the C2′−N1′ bond as described in preceding section. It should be noted that a second pathway, less energetically favorable and involving an inversion mechanism at the nitrogen N1′, connects the s-cis with the merocyanine forms.[18] This pathway has already been described elsewhere and will be not considered here.[18]

3.3.2.4. S_2 PES. It remains to be shown how the S_1 surface is reached from the second excited singlet state S_2. The energetic evolution of the S_2 singlet excited state as the C−O bond is elongated is also reported in Figure 5b (TD-DFT calculations). Following the gradient in the Franck−Condon region, a shallow S_2 minimum at geometry S_2-CF(R) is reached. However, due to the small gap between the S_2 and S_1 excited state, avoided crossing occurs at a short C−O bond distance and the S_1 state becomes a $\pi-\pi^*$ state localized on the naphthoxazine part. After this first avoided crossing, the S_1 state before the excited energy barrier is essentially a $\pi-\pi^*$ CT state. But the electronic structure of the S_1 state (mostly a $\pi-\pi^*$ LE state) at the conical intersection suggests that the excited transition state corresponds to an avoided crossing with an upper state. This avoided crossing is caused by the single C−O bond elongation and the rapid decreasing of the energy of the corresponding σ^*_{CO} orbital. The major changes in the wave function correspond to a decreasing contribution of the $\Phi_{H\rightarrow L}$ ($\pi \rightarrow \pi^*$ contribution localized on the naphthoxazine part) and increasing of the $\Phi_{\pi\rightarrow\sigma^*}$ (with σ^* localized on the C−O bond). Initially, the $\pi \rightarrow \pi^*$ configuration dominates the S_1 state (0.51) while the $\pi \rightarrow \sigma_{CO}^*$ dominates the S_1 state (0.68) after the ring opening. This verifies the existence of an avoided crossing as the origin of the fast internal conversion to the first excited state. The change from the $\pi-\pi^*$ (located on the naphthalene moiety) to the $\eta-\pi^*$ electronic configuration is driven by the $C_2-O_{4'}$ breaking.

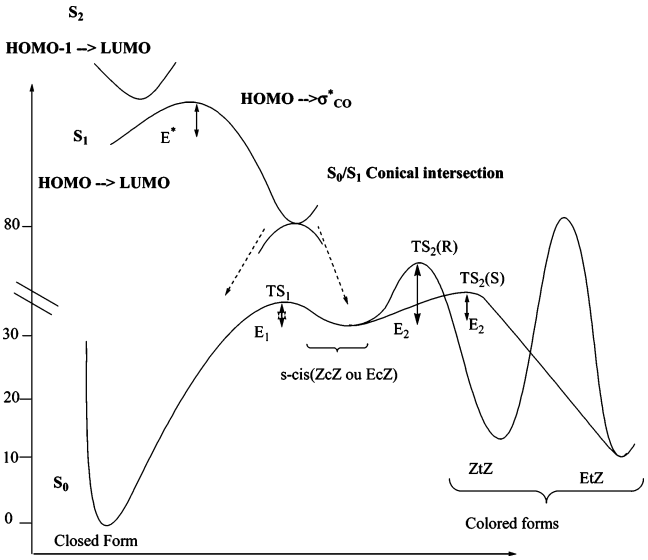

Figure 9. Schematic representation of the ground and excited PES for the ring-opening reaction of SNO.

The computational data presented above suggest an efficient decay path from S_1 to the merocyanine ground-state form. A schematic overview of the SNO ring-opening path obtained from our calculations is displayed in Figure 9.

In summary, excitation leading the S_2 state ($\pi-\pi^*$ naphthoxazine-localized state), an avoided crossing occurs between the S_1 and S_2 excited-states energy surfaces for very short C−O bond elongation (d(C−O) = 1.6 Å). Then, the initially S_1 π-(indoline)$-\pi^*$(naphthoxazine) CT state becomes a $\pi-\pi^*$ state localized on naphthoxazine. Then, the system relaxes to the ground-state S_0 through a conical intersection from which deactivation toward the initial closed form or s-cis intermediate is possible. The s-cis isomer has an energy minimum in a basin surrounded by TS(s-cis → CF) and TS(s-cis → merocyanine). For the ZcZ isomer, the barrier of reformation of the spiro compound is lower (2.3 kcal·mol^{-1}) than that of rotation (11.2 kcal·mol^{-1}) to the corresponding colored ZtZ isomer. Therefore, the ring-opening reaction from the spiro CF(R) compound is expected to lead exclusively to the initial closed form and only a little fraction of open colored isomer is expected to be produced via this mechanism. For the EcZ isomer the two barriers are almost equal (less than 2 kcal·mol^{-1}), and much amount of merocyanine EtZ should be produced. This result seems to agree well with time-resolved Raman spectroscopy which concluded to the formation of a mixture of EtZ and ZtZ forms at very short time (less than 10 ps) but with a dominant of EtZ isomeric structure.[15]

This model of excited ring opening provides a simple explanation for various experimental features. The observed ∼0.4 (the quantum yield of photocoloration of SNO only weakly depends on the solvent and is found ranging from 0.3 in a polar solvent such acetonitrile to 0.4 in methylcyclohexane) ring-opening quantum yield of photocoloration is consistent with ground-state bifurcation which leads to competitive formation of the s-cis isomer and back-formation of the original reactant

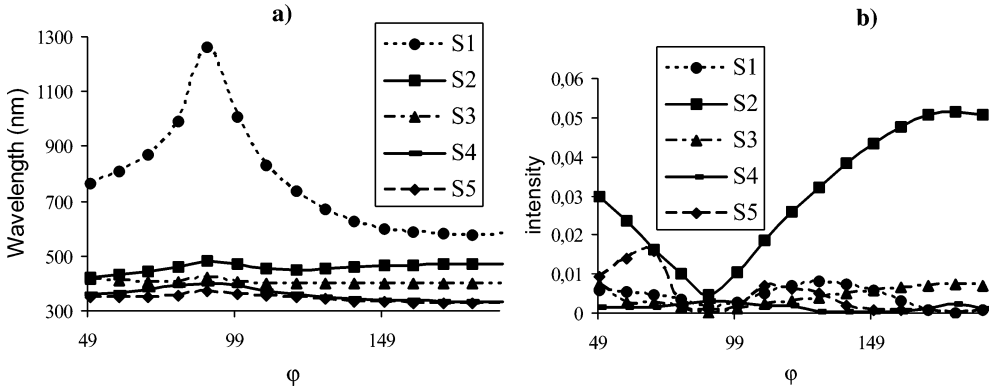

Figure 10. Evolution of the energies (a) and intensities (b) of the first five excited states as a function of the torsional angle φ (φ varies from 49° to 180° corresponding to the value in the EcZ and EtZ isomers, respectively).

(closed form). In addition, the computed low energy barrier for ring opening in the first singlet excited state is consistent with the femtosecond appearance time measured for the first photoproduct, i.e., s-cis, and also consistent with the lack of fluorescence (even at low temperature) for SNO. Furthermore, it can be noted that the s-cis isomer, having a structure similar to that of the initial spiro form, is reported to be the first photoproduct in the photochromism of spirobenzopyran.[44] It should be kept in mind that the results of calculations cannot be directly compared to the experimental data obtained in condensed medium. However, although the molecular calculations are performed for the isolated system, these calculations probably reflect the reactivity of the system in an apolar solvent. The key point of our results is that the s-cis isomers (ZcZ and EcZ) play a specific role in the photoreaction leading to the merocyanines (colored) species (ZtZ and EtZ, respectively). One can note, however, that the ground-state surface displayed in our results fails to explain the reaction speed of photocoloration which was measured by experiments in the picosecond time range. Indeed, starting from the s-cis isomer, the barrier of isomerization is much higher than the energy barrier for ring closing. Therefore, the yield of the process from the equilibrated s-cis isomer should be negligible. Several reasons could explain this insufficiency. First, it must be pointed out that the calculations undertaken do not take account of the thermochemical corrections, and it can be anticipated that the entropic factor disadvantages the ring-closing reaction while the cis−trans process must be favored. Thermodynamic parameters such as Gibbs free energy were calculated at the B3LYP/6-31G(d) level of theory by frequencies calculations. Briefly and from the ZcZ isomer, the entropic factor increases the energy barrier for ring closure from 2.3 to 3.0 kcal·mol^{-1}, while the cis−trans energy barrier decreases from 11.2 to 8.5 kcal·mol^{-1}. Starting from the EcZ isomer, the Gibbs free energy barriers of activation for the ring closure and cis−trans reactions are almost the same, i.e., 1.7 and 2.3 kcal·mol^{-1}, respectively. Second, the barrier of cis−trans energy strongly depends on the effect of correlation, and the cis−trans process occurs without barrier of energy at the Hartree−Fock level of calculation (HF/6-31G(d) calculations, not shown). The systematic study with various correlated methods should make it possible to clarify this point. Finally, it could be also mentioned that the ground-state species formed from photoreaction is rich in vibrational energy and that from the outset it can reach the basin of the trans form.

3.4. Spectrum Evolution in the Course of the Photocoloration. To provide some comparative data with the experiments obtained in nonpolar solvent, the UV−vis absorption spectra of SNO after the ring-opening reaction are calculated by TD-DFT with the 6-31G basis set. The structures of SNO are taken from the optimized geometries obtained on the ground-state ring-opening pathway and calculated with the B3LYP/6-31G(d) method. On the basis of experimental results, we assume that the C−O bond cleavage leading to the s-cis isomer is very fast and takes place in only a few hundred of femtoseconds. Therefore, most of the time evolution of the UV−vis absorption spectra is a fingerprint of the ground-state s-cis−merocyanine isomerization. We calculated the first five lowest excitation energies using TD-DFT as a function of the twist angle φ around the C2′−N1′ bond. The geometries were taken from the ground-state minimum energy reaction path obtained in the previous section. The calculations for isomerization of ZcZ and EcZ are very similar in all aspects. Therefore, the calculations of the ZcZ isomerization are not reported, as it does not offer any significantly different behavior. The excitation energies for the twisting starting from the EcZ isomer as well as the intensity are reported in Figure 10, parts a and b, respectively. In general, the lowest state S_2 always has the largest transition probability, while the other lowest states have very weak intensities. The energy of S_2 only slightly decreases as the two moieties of the molecule twist, and at the same time the intensity decreases, and at $\theta = 90°$, it becomes almost a forbidden transition.

Using the lowest five excitations, we plot the UV−vis spectra for each value of dihedral angle, i.e., C3′−C2′−N1′−C11′, corresponding to the thermal cis−trans isomerization (Figure 11). Each excitation is expressed as a weighted Gaussian centered at the excitation energy with a half-bandwidth of 0.5 eV; weights are directly proportional to the oscillator strengths.[45]

For a small dihedral angle, a maximum absorption is calculated near 450 nm. There is a red shift in the absorption as the molecule rotates around the C−N bond until a value of 90°. From 90°, as the dihedral angle increases to reach the value of 180°, the molecule becomes more planar and the maximum absorption smoothly shifts to the long-wavelength region while the intensity strongly increases. These evolutions are in good agreement with those observed using time-resolved spectroscopy techniques in a nonpolar solvent such as cyclohexane.[12] Thus, the results of calculations suggest that the evolution of the spectra observed after a few picoseconds, in particular the red shift and strong increase in the intensity of the maximum absorption peak as well as the decreasing of the half-bandwidth of this maximum, are compatible with conformation rearrangement of the cis−trans type.

3.5. Quantum Yield of Photocoloration: Correlation between Experimental and Calculated Properties. The mechanism of ring opening deduced from theoretical calculations has shown that the first photoproduct obtained along the ring-opening pathway should be the s-cis intermediate. This species can rearrange through cis−trans isomerization leading to

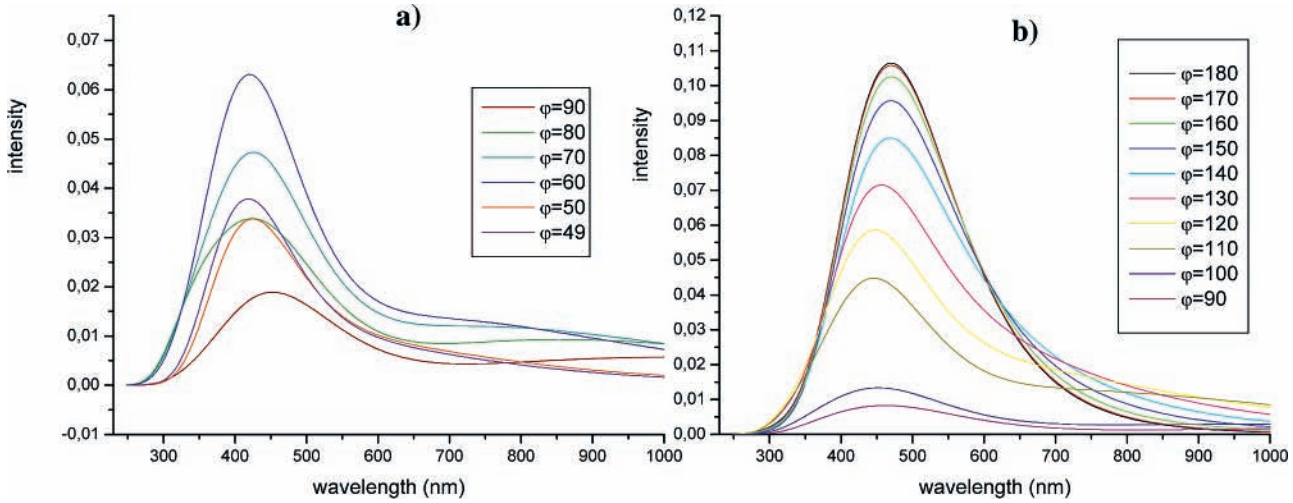

Figure 11. UV−vis spectra of SNO as a function of the torsional angle φ (cis−trans isomerization): (a) 49° < φ < 90°; (b) 90° < φ < 180°.

TABLE 4: Experimental Quantum Yield of Photocoloration ϕ_{col} and Calculated Energies Barrier E_1 (ZcZ → CF) and E_2 (ZcZ → ZtZ) Isomerizations (in kcal·mol^{-1}) for the Unsubstituted (1) Compound and Substituted (2−7) Compounds

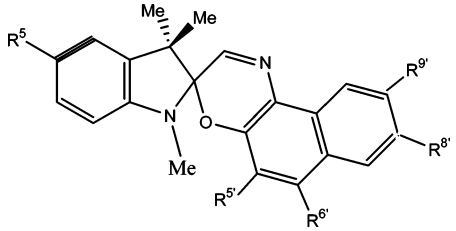

compound	R^5	$R^{5'}$	$R^{6'}$	$R^{8'}$	$R^{9'}$	ϕ_{col}[a,b]	E_1 (ZcZ → CF)[c]	E_2 (ZcZ → ZtZ)[c]
1	−H	−H	−H	−H	−H	0.33	1.2	11.2
2	−H	−CH═CH−CN	−H	−H	−H	0.124	0.9	15.0
3	−H	−H	$-NC_5H_{10}$[d]	−H	−H	0.477	1.7	8.6
4	−H	−H	−CN	−H	−H	0.171	0.6	13.9
5	$-OCH_3$	−H	−CN	−H	−H	0.106	0.5	15.2
6	$-OCH_3$	−H	−H	−CN	−H	0.137	0.5	15.0
7	−H	−H	−H	−H	$-OCH_3$	0.356	1.4	10.3

[a] In toluene. [b] Ref 46. [c] B3LYP/6-31G calculations. [d] Piperidino substituent.

merocyanine or via ring-closure reaction to the initial closed form. Therefore, just after the UV excitation, almost half of the molecules rapidly reach the s-cis minimum of the ground-state PES. The other amount of molecules reverts back to the initial closed form. From the s-cis isomer the molecule can evolve toward the corresponding merocyanine or can also revert back to the closed form. Therefore, when the s-cis region is populated, the quantum yield efficiency of photocoloration will depend on the ability of the system to overcome the energy barrier between the s-cis and s-trans compared to the energy barrier for the return toward the closed form. The presence of substituents should affect the energy barrier and may influence the quantum yield. To test the validity of this hypothesis, we carried out further calculations of the energy barrier for cis−trans isomerization, E_2, and ring closure, E_1, from the s-cis isomer and for various derivatives whose experimental quantum yields of photocoloration, ϕ_{col}, are known (Table 4).[46] Although the most probable pathway leading to the merocyanine isomer involves the EcZ isomer, through EcZ → EtZ isomerization, calculations were restricted to the ZcZ → ZtZ energy barrier. Indeed, the EcZ → EtZ energy barrier is in general very low and even disappears for some compounds. It could be noted that the distribution of EtZ and ZtZ was detected in NOE experiments and using ^{1}H NMR spectroscopy at low temperature for the unsubstituted molecule (SNO).[38] Furthermore, these experiments were carried out in polar solvents (methanol and acetonitrile). Thus, the distribution of ZtZ and EtZ isomers might be different in nonpolar solvents and also might change the nature of the substituent. Seven compounds have been selected for the calculation, and the corresponding energies barriers ($E_1 = E(TS_{C-O}) - E(ZcZ)$ and $E_2 = E(TS_{ZcZ\rightarrow ZtZ}) - E(ZcZ)$) are listed in Table 4.

The highest ϕ_{col} is obtained when the piperidino group is in position 6′ (compound 3, $\phi_{col} = 0.477$), while the lowest ϕ_{col} is obtained with −CN in position 6′ (compound 5, $\phi_{col} = 0.106$). One can first note that the calculated barrier of cyclo-reversion, ZcZ → CF, is small and does not change significantly upon substitution (from 0.5 to 1.7 for compounds 6 and 3, respectively) while the ZcZ → ZtZ energy barrier is considerably higher and much more sensitive to substitution. This means that the quantum yield of photocoloration will mostly depend on the cis−trans isomerization barrier. A higher quantum yield is associated with a lower E_2 (compound 3). On the contrary, with the −CN substituent in the 6′ position, the highest E_2 (compound 5) is obtained. The correlation between experimental quantum yields and calculated E_2 is shown in Figure 12. A very good correlation is obtained indicating that the s-cis−trans energy

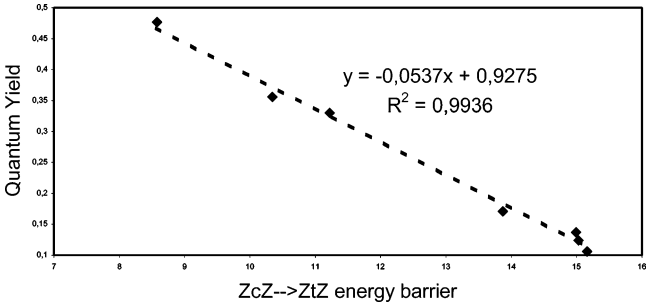

Figure 12. Correlation of the experimental quantum yield of photocoloration with the calculated ZcZ → ZtZ energy barrier, E_2.

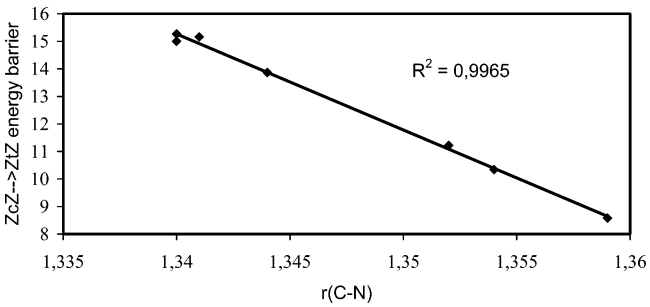

Figure 13. Correlation of the calculated E_2 energy barrier (in kcal·mol^{-1}) with the optimized C−N bond distance (in Å) in ZcZ.

barrier is an important parameter in controlling the photocoloration reaction.

The nature of the cis−trans isomerization barrier may be projected in the strength of the C2′−N1′ bond in the s-cis isomer. At first glance, the strength of the C2′−N1′ bond can be related to the C2′−N1′ bond distance. In fact, the calculated energy barriers and C2′−N1′ optimized bond distances in the s-cis isomer show a very good correlation as shown in Figure 13.

We are aware that many approximations underlie our approach, and several other factors can control the quantum yield of photocoloration. For example, a recent study has demonstrated the importance of intramolecular vibrational redistribution in the ring-opening reactions.[47] However, this correlation can be useful in practice as the weakness of C−N bond will lead to a higher quantum yield, while opposite effect will be observed if the C−N bond is stronger.

4. Conclusion

In this study, we calculated the ring-opening energy profile for SNO in the ground and excited states. The information obtained in different regions of the excited energy surface is consistent with the following view: (i) The electronic transition to the S_2 state will carry most of the excitation energy due to the strongly dipole-allowed Franck−Condon character. (ii) Deactivation to the S_1 state occurs, and the oxazine cycle opens with a low barrier of activation. The molecule reaches a conical intersection where fast decay to the ground surface leads to either the initial closed form or the s-cis opened form. (iii) The colored merocyanines are then obtained by cis−trans isomerization. Energetic consideration leads to the conclusion that the ZcZ isomer should revert mainly to the closed form CF(R) instead of giving the ZtZ colored photoproduct. Therefore, the merocyanine colored form is obtained mainly by cis−trans isomerization from the EcZ isomer. The barrier of the cis−trans isomerization is found to have a strong influence on the efficiency of the photocoloration process. This result offers a qualitative guide to improve the quantum yield of photocoloration and the synthesis of new photochromic compounds.

References and Notes

(1) (a) Bertelson, R. C. In *Photochromism*; Brown, G. H., Ed.; Techniques in Chemistry; Wiley-Interscience: New York, 1971; Vol. 3, p 45. (b) *Photochromism: Molecules & Systems*; Durr, H., Bouas-Laurent, H., Eds.; Elsevier: New York, 1990.

(2) *Organic Photochromic and Thermochromic Compounds*; Crano, J. C., Guglielmetti, R. J., Eds.; Kluwer Academic/Plenum Publishers: New York, 1999.

(3) Chu, N. Y. C. In *Photochromism: Molecules & Systems*; Durr, H., Bouas-Laurent, H., Eds.; Elsevier: New York, 1990; p 493.

(4) Maeda, S. In *Organic Photochromic and Thermochromic Compounds*; Crano, J. C., Guglielmetti, R. J., Eds.; Kluwer Academic/Plenum Publishers: New York, 1999; Vol. 1, pp 85−109.

(5) Crano, J. C.; Kwak, W. S.; Welch, C. N. *Applied Photochromic Polymer Systems*; McArdle, C. B., Ed.; Blackie: London, 1992; Chapter 2, p 31.

(6) Berkovic, G.; Krongauz, V.; Weiss, V. *Chem. Rev.* **2000**, *100*, 1741.

(7) Samat, A.; Lokshin, V. In *Organic Photochromic and Thermochromic Compounds*; Crano, J. C., Guglielmetti, R. J., Eds.; Kluwer Academic/Plenum Publishers: New York, 1999; Vol. 2, p 415.

(8) Kellmann, A.; Tfibel, F.; Dubest, R.; Levoir, P.; Aubard, J.; Pottier, E.; Guglielmetti, R. *J. Photochem. Photobiol., A* **1989**, *49*, 63.

(9) Schneider, S. *Z. Phys. Chem.* **1987**, *154*, 91.

(10) Wilkinson, F.; Worarall, D. R.; Hobley, J.; Jancsen, L.; Williams, S. L.; Langley, A. J.; Matousek, P. *J. Chem. Soc., Faraday Trans.* **1996**, *92*, 1331.

(11) Tamai, N.; Masuhara, H. *Chem. Phys. Lett.* **1992**, *191*, 189.

(12) Antipin, S. A.; Petrukhin, A. N.; Gostev, F. E.; Marevtsev, V. S.; Titov, A. A.; Barachevsky, V. A.; Strokach, Yu. P.; Sarkisov, O. M. *Chem. Phys. Lett.* **2000**, *331*, 378.

(13) Aubard, J.; Maurel, F.; Buntinx, G.; Poizat, O.; Lévi, G.; Guglielmetti, R.; Samat, A. *Mol. Cryst. Liq. Cryst.* **2000**, *345*, 215.

(14) Aramaki, S.; Atkinson, G. H. *Chem. Phys. Lett.* **1990**, *170*, 181.

(15) Aubard, J.; Maurel, F.; Buntinx, G.; Guglielmetti, R.; Lévi, G. *Mol. Cryst. Liq. Cryst.* **2000**, *345*, 203.

(16) Aubard, J. In *Organic Photochromic and Thermochromic Compounds*; Crano, J. C., Guglielmetti, R. J., Eds.; Kluwer Academic/Plenum Publishers: New York, 1999; Vol. 2, pp 357−392.

(17) Nakamura, S.; Uchida, K.; Murakami, A.; Irie, M. *J. Org. Chem.* **1993**, *58*, 5543.

(18) Maurel, F.; Aubard, J.; Rajzmann, M.; Guglielmetti, R.; Samat, A. *J. Chem. Soc., Perkin Trans. 2* **2002**, 1307.

(19) Celani, P.; Bernardi, F.; Olivucci, M.; Robb, M. A. *J. Am. Chem. Soc.* **1997**, *119*, 10815.

(20) Frisch, M. J.; Trucks, G. W.; Schlegel, H. B.; Scuseria, G. E.; Robb, M. A.; Cheeseman, J. R.; Zakrzewski, V. G.; Montgomery, J. A.; Stratmann, R. E.; Burant, J. C.; Dapprich, S.; Millam, J. M.; Daniels, A. D.; Kudin, K. N.; Strain, M. C.; Farkas, O.; Tomasi, J.; Barone, V.; Cossi, M.; Cammi, R.; Mennucci, B.; Pomelli, C.; Adamo, C.; Clifford, S.; Ochterski, J.; Petersson, G. A.; Ayala, P. Y.; Cui, Q.; Morokuma, K.; Malick, D. K.; Rabuck, A. D.; Raghavachari, K.; Foresman, J. B.; Cioslowski, J.; Ortiz, J. V.; Stefanov, B. B.; Liu, G.; Liashenko, A.; Piskorz, P.; Komaromi, I.; Gomperts, R.; Martin, R. L.; Fox, D. J.; Keith, T.; Al-Laham, M. A.; Peng, C. Y.; Nanayakkara, A.; Gonzalez, C.; Challacombe, M.; Gill, P. M. W.; Johnson, B. G.; Chen, W.; Wong, M. W.; Andres, J. L.; Head-Gordon, M.; Replogle, E. S.; Pople, J. A. *Gaussian 98*, revision A.1; Gaussian, Inc.: Pittsburgh, PA, 1998.

(21) König, G.; Stollhoff, G. *Phys. Rev. Lett.* **1990**, *65*, 1239.

(22) (a) Becke, A. D. *J. Chem. Phys.* **1993**, *98*, 5648. (b) Lee, C.; Yang, W.; Parr, R. G. *Phys. Rev. B* **1988**, *37*, 785.

(23) (a) Hariharan, P. C.; Pople, J. A. *Chem. Phys. Lett.* **1972**, *66*, 217. (b) Hehre, W. J.; Radom, L.; Schleyer, P. v. R.; Pople, J. A. *Ab Initio Molecular Orbital Theory*; Wiley: New York, 1986.

(24) Dewar, M. J. S.; Zoebish, E. G.; Healy, E. F.; Stewart, J. J. P. *J. Am. Chem. Soc.* **1985**, *107*, 3902.

(25) *AMPAC 7.0 Code*; Semichem, Inc.: Shawnes, KS 1992−2003.

(26) (a) Agmon, A.; Rettig, W.; Groth, C. *J. Am. Chem. Soc.* **2002**, *124*, 1089. (b) Gedeck, P.; Schneider, S. *J. Photochem. Photobiol., A* **1999**, *121*, 7. (c) Lambert, C.; Risko, C.; Coropceanu, V.; Schelter, J.; Amthor, S.; Gruhn, N. E.; Durivage, J. C.; Bredas, J. L. *J. Am. Chem. Soc.* **2005**, *127*, 8508.

(27) (a) Mommicchioli, F.; Baraldi, I.; Bruni, M. C. *Chem. Phys.* **1982**, *70*, 161. (b) Mommicchioli, F.; Baraldi, I.; Bruni, M. C. *Chem. Phys.* **1983**, *82*, 229.

(28) Huron, B.; Malrieu, J. P.; Rancurel, P. J. *Chem. Phys.* **1973**, *58*, 5745.

(29) Germain, A.; Millie, P. *Chem. Phys.* **1997**, *219*, 265.

(30) Maurel, F.; Samat, A.; Guglielmetti, R.; Aubard, J. *Mol. Cryst. Liq. Cryst.* **2000**, *345*, 75.

(31) (a) Bauernschmitt, R.; Ahlrichs, R. *Chem. Phys. Lett.* **1996**, *256*, 454. (b) Casida, M. E.; Jamorski, C.; Casida, K. C.; Salahub, D. R. *J. Chem. Phys.* **1998**, *108*, 4439. (c) Stratman, R. E.; Scuseria, G. E.; Frisch, M. J. *J. Chem. Phys.* **1998**, *109*, 8218.

(32) (a) Tyer, N. W., Jr.; Becker, R. S. *J. Am. Chem. Soc.* **1970**, *92*, 1289. (b) Tyer, N. W., Jr.; Becker, R. S. *J. Am. Chem. Soc.* **1970**, *92*, 1295.

(33) Ernsting, N. P.; Arthen-Engeland, Th. *J. Phys. Chem.* **1991**, *95*, 5502.

(34) Slaughter, B. D.; Allen, M. W.; Lushington, G. H.; Johnson, K. *J. Phys. Chem. A* **2003**, *170*, 5670.

(35) Del Bene, J. E. *Chem. Phys. Lett.* **1976**, *44*, 512.

(36) Zyubin, A. S.; Mebel, A. M. *J. Comput. Chem.* **2003**, *24*, 692.

(37) Barone, V.; Cossi, M. *J. Phys. Chem. A* **1998**, *102*, 1995.

(38) Delbaere, S.; Bochu, C.; Azaroual, N.; Buntinx, G.; Vermeersch, G. *J. Chem. Soc., Perkin Trans. 2* **1997**, 1499.

(39) (a) Sheng, Y.; Lesczczynski, J.; Garcia, A. A.; Rosario, R.; Gust, D.; Springer, J. *J. Phys. Chem. B* **2004**, *108*, 16233. (b) Minkin, V.; Metelitsa, A. V.; Dorognan, I. V.; Lukyanov, B. S.; Besugliy, S. O.; Micheau, J.-C. *J. Phys. Chem. A* **2005**, *109*, 9605.

(40) Millini, R.; Del Piero, G.; Allegrini, P.; Crisci, L.; Malatesta, V. *Acta Crystallogr., Sect. C* **1991**, *47*, 2567.

(41) Bohne, C.; Fan, M. G.; Li, Z. J.; Luszlyk, J.; Scaiano, J. C. *J. Chem Soc., Chem. Commun.* **1990**, 571.

(42) Chibisov, A. K.; Marevtsev, V. S.; Görner, H. J. *Photochem. Photobiol.* **2003**, *159*, 233.

(43) (a) Zheng-Li, C.; Reimers, J. R. *J. Chem. Phys.* **2000**, *112*, 527−530. (b) Zheng-Li, C.; Tozer, D. J.; Reimers, J. R. *J. Chem. Phys.* **2000**, *112*, 7084.

(44) Chibisov, A. K.; Görner, H. *J. Phys. Chem. A* **1997**, *101*, 4305.

(45) Pearl, G. M.; Zerner, M. C.; Broo, A.; McKelvey, J. *J. Comput. Chem.* **1998**, *19*, 781.

(46) Metelitsa, A. V.; Lokshin, V.; Micheau, J. C.; Samat, A.; Guglielmetti, R.; Minkin, V. I. *Phys. Chem. Chem. Phys.* **2002**, *18*, 4340.

(47) Migani, A.; Gentili, P. L.; Negri, F.; Olivucci, M.; Romani, A.; Favaro, G.; Becker, R. S. *J. Phys. Chem. A* **2005**, *109*, 8684.